

Pixel Super Resolution with Axial Scanning in Lensless Digital In-line Holographic Microscopy

Karolina Niedziela*, Mikołaj Rogalski, Piotr Arcab, Julianna Winnik, Piotr Zdańkowski, Maciej Trusiak†

Faculty of Mechatronics, Warsaw University of Technology, św. Andrzeja Boboli 8, 02-525 Warszawa

Received November 28, 2008; accepted December 4, 2008; published December 5, 2008

Abstract— This paper presents the Pixel Super Resolution with Axial Scanning (PSR-AS) technique to enhance the resolution of Lensless Digital In-line Holographic Microscopy (LDHM). By utilizing multiple holograms captured at different axial distances, PSR allows for the recovery of high-resolution information, improving image clarity and information content. Experimental results demonstrate a twofold lateral resolution enhancement, achieving the resolution of $1.23\ \mu\text{m}$ in amplitude imaging and significantly augmenting phase reconstruction quality. Integrating PSR-AS into LDHM systems leads to notable reductions in noise and artifacts, offering a promising approach for high-resolution imaging in applications such as biomedical diagnostics and environmental monitoring.

Quantitative phase imaging (QPI) is a technique for visualizing transparent specimens by capturing phase information, which is crucial for applications in cell biology, material science, and biomedical diagnostics [1]. Among QPI methods, lensless digital in-line holographic microscopy (LDHM) provides a cost-effective and efficient solution. Unlike traditional microscopy, LDHM eliminates optical lenses and uses computational techniques to reconstruct images from light diffraction patterns. The basic configuration of an LDHM system consists of a camera, a light source (typically a laser), and a sample, Fig. 1. Based on holographic principles introduced by Dennis Gabor in 1948 [2], LDHM involves illuminating a semi-transparent specimen with a coherent or partially coherent light source. The diffracted light interferes with a reference unscattered wave to produce an interference pattern (in-line hologram) on the sensor. Numerical backpropagation methods, such as the angular spectrum method (ASM), are used to reconstruct the optical field, extracting optical thickness and structural data of the specimen [3]. Despite lacking traditional optics, LDHM enables decent-resolution imaging with large fields of view and significant depth of focus, making it suitable for biomedical diagnostics, environmental monitoring, and point-of-care applications [4]. In summary, LDHM combines simplicity, cost-efficiency, and powerful imaging capabilities, offering a promising alternative to conventional microscopy.

LDHM faces two key limitations: (1) twin-image noise, resulting from lack of phase factor in acquired in-line holograms [4], and (2) moderate spatial resolution, limited primarily by pixel size, and other factors such as sensor

size, coherence of the illumination, computational reconstruction errors, and noise in the recorded diffraction patterns [5]. One common approach to mitigate twin image artifacts in LDHM involves capturing multiple axially spaced holograms and applying the Gerchberg-Saxton (GS) algorithm [6] for phase retrieval. To further enhance resolution, pixel super-resolution (PSR) algorithms are often employed, typically requiring sub-pixel-level XY scanning to numerically reduce the effective pixel size [7]. However, combining PSR with GS often demands the acquisition of a substantial number of holograms, which can be computationally and experimentally burdensome [8]. Interestingly, recent studies, such as [9], suggest that PSR can be incorporated directly within the iterative GS framework, significantly reducing the required number of holograms.

In this work, we demonstrate that this combined PSR-AS (Pixel Super Resolution with Axial Scanning) approach can achieve a twofold resolution improvement and twin image reduction for both amplitude and phase imaging. Our results showcase the feasibility of achieving high-resolution imaging in LDHM systems while maintaining a large FOV, further positioning this technology as a promising tool for diverse imaging applications.

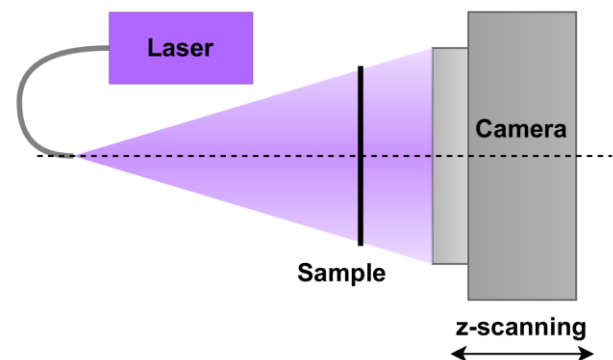


Fig. 1. Scheme of the laboratory setup.

Building on the principles outlined earlier, we now explore the specifics of the PSR-AS algorithm. The method utilizes multiple holograms captured at different defocus distances to iteratively reconstruct a high-resolution optical field. The input data consists of holograms, recorded as

* E-mail: karolina.niedziela.stud@pw.edu.pl

† E-mail: maciej.trusiak@pw.edu.pl

intensity maps, along with metadata, including propagation distances, illumination wavelength, and the detector's pixel size. The algorithm relies on iterative propagation between hologram and object planes. Starting with the amplitude of the first hologram, the field is propagated to the object planes of subsequent holograms using ASM [3]. At each step, the up-sampled propagated field is down-sampled, updated by blending it with the intensity data of the corresponding hologram, and then up-sampled [9]. In other words, the algorithm looks for the up-sampled optical field solution that fits the coarsely sampled defocused intensity observations. To improve reconstruction accuracy, additional filtering, such as total variation denoising [10], can be applied to suppress noise. After processing all holograms, the field is propagated back to the object plane to reconstruct high-resolution in-focus object amplitude-phase information.

In the next part, we present the experimental results obtained from the PSR-AS LDHM. The laboratory optical setup consists of single-mode optical fiber with a solid-state laser source (CNI Lasers MDL-III-405-20 mW, $\lambda = 405$ nm) and a camera (Alvium 1800 U-2050) with a pixel size of $2.4 \mu\text{m}$ (Fig. 1). Firstly, we investigate the proposed method on the amplitude-type USAF resolution test target, with the results presented in Fig. 2, demonstrating significant resolution improvements that enhance the clarity and detail of the target. Images in Figs. 2(b) and 2(e) represent the reconstructions of a single hologram via ASM, spoiled with the twin image artifacts and exhibiting modest unmodified lateral resolution. The smallest resolvable detail corresponds to a resolution of $2.46 \mu\text{m}$ (group 7, element 5), thus very close to 2.4 -micron pixel size. Images in Figs. 2(c) and 2(f) represent the reconstructions obtained with a multi-height GS [6] algorithm from 10 holograms collected at different camera-sample distances. We can see that the GS method effectively removes twin-image artifacts and suppresses noise. However, there is no improvement in resolution. Images in Figs. 2(d) and 2(g) demonstrate the reconstruction after a PSR-AS algorithm with an up-sampling factor of 4, significantly improving resolution and the clarity of the finest details. The smallest resolvable detail corresponds to a resolution of $1.23 \mu\text{m}$ (group 8, element 5), representing a twofold enhancement in lateral resolution compared to the initial reconstruction.

The next imaged object is a phase test target, etched to a depth of 125 nm, with the smallest transverse element dimension of $2 \mu\text{m}$, and its full FOV hologram is presented in Fig. 3(a). The red square drawn on the top image highlights the test area with the finest transverse resolution details, group S. Figures 3(b)-3(d) show the phase reconstruction results in group S of the phase test target with the ASM (single hologram), GS (5 holograms) and PSR-AS (5 holograms) methods respectively. We can see that the twin image artifacts (manifested as diffraction fringes around the measured object) are significantly

reduced with GS and 4-fold PSR-AS methods compared to the ASM.

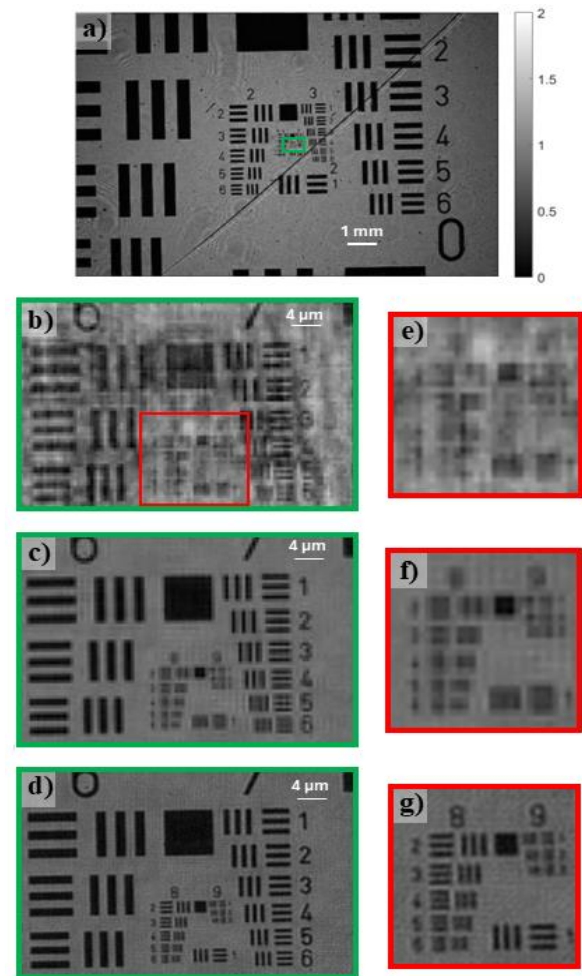


Fig. 2. Amplitude reconstruction results of an amplitude USAF test target: (a) – full FOV of an amplitude USAF test target, (b, c, d) – enlarged green rectangle regions of (a), (e, f, g) – enlarged red square regions of (b, c, d), (b, e) – a single hologram reconstruction without PSR, (c, f) – GS reconstruction with 10 holograms, (d, g) – reconstruction with 4-fold PSR-AS with 10 holograms.

The images with green outlines Figs. 3(e)-3(g) show the enlarged region of Figs. 3(b)-3(d), respectively, with phase reconstruction results obtained deploying the mentioned algorithms. The phase variations across these reconstructions provide insights into the reconstruction quality and the influence of super-resolution techniques. In single hologram ASM reconstruction, Fig. 3(e), we can see that the phase reconstruction contains some artifacts in the background, and the presence of the noise is obvious. In GS reconstruction, Fig. 3(f), the phase reconstruction becomes much clearer, but the lines are still not resolvable due to the generally too modest lateral resolution. In PSR-AS reconstruction, Fig. 3(g), the phase accuracy is comparable with the GS method; however, the reconstruction lateral resolution is significantly improved

– the test elements from group S (corresponding to a resolution of 2 μm) become easily resolvable.

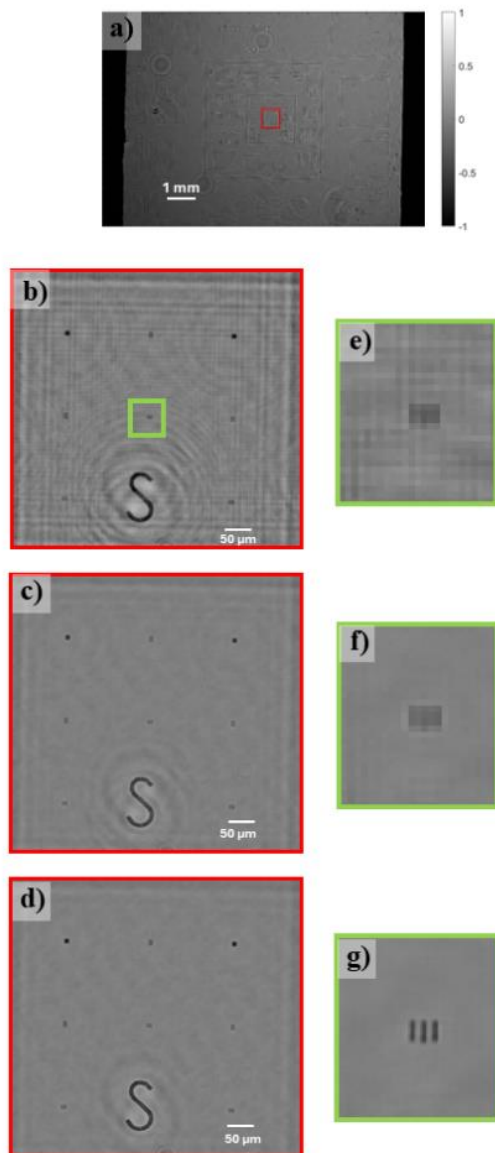


Fig. 3. Phase reconstruction results of a phase test target: (a) full FOV of a phase test target; (b–d) enlarged red square regions of (a); (e–g) enlarged green rectangle region of (b,c,d); (b, e) single hologram reconstruction without PSR-AS; (c, f) GS reconstruction with 5 holograms; (d, g) reconstruction with 4-fold PSR-AS with 5 holograms.

In this paper, we have presented the PSR-AS technique as an effective solution to overcome the resolution limitations in lensless holographic imaging systems due to physical pixel size. By utilizing multiple holograms at different propagation distances, the PSR-AS algorithm recovers high-resolution information, numerically pushing LDHM systems closer to the diffraction limit. Experimental results show that the PSR-AS algorithm significantly enhances resolution in both amplitude and phase imaging. Specifically, a 4-fold PSR-AS with 10

holograms led to a twofold lateral resolution improvement compared to single hologram reconstructions, achieving the smallest resolvable detail of 1.23 μm . This enhancement was especially evident in the USAF test target images, where fine details became visible, and noise and twin-image artifacts inherent in LDHM were reduced. Additionally, phase test target results demonstrated the PSR-AS algorithm's ability to improve phase imaging quality, making previously indistinguishable features resolvable. The integration of PSR-AS into the LDHM setup with a 405 nm laser and high-resolution camera marks a significant advance in lensless microscopy, offering substantial improvements in clarity and resolution. This work highlights the potential of PSR-AS for high-resolution applications, particularly in biomedical diagnostics and environmental monitoring. In conclusion, PSR-AS proves to be an effective method for enhancing the resolution of lensless holographic microscopy systems, offering promise for future research and practical applications.

Studies were funded by Young PW projects granted by Warsaw University of Technology under the program Excellence Initiative: Research University (ID-UB) in POB Photonic Technologies.

Partially funded by the European Union (ERC, NaNoLens, Project 101117392). Views and opinions expressed are, however, those of the author(s) only and do not necessarily reflect those of the European Union or the European Research Council Executive Agency (ERCEA). Neither the European Union nor the granting authority can be held responsible for them.

References

- [1] Y. Park, C. Depeursinge, G. Popescu, *Nature Photon.* **12**(10), 578 (2018); doi: 10.1038/s41566-018-0253-x
- [2] D. Gabor, *Nature* **161**(4098), 777 (1948); doi: 10.1038/161777a0
- [3] K. Matushima, T. Shimobaba, *Opt. Express* **17**(22), 19662 (2009); doi: 10.1364/OE.17.019662
- [4] Y. Wu, A. Ozcan, *Methods* **136**, 4 (2018); doi:10.1016/j.jymeth.2017.08.013
- [5] J. Zhang, J. Sun, Q. Chen, C. Zuo, *IEEE Transact. Comput. Imaging* **6**, 697 (2020), doi: 10.1109/TCI.2020.2964247
- [6] R. Gerchberg, W.O. Saxton, *SPIE milestone series MS 94* (1994): 646-646.
- [7] H. Lee, J. Kim, J. Kim, P. Jeon, S.A. Lee, D. Kim, *Opt. Express* **29**(19), 29996 (2021); doi: 10.1364/OE.433719
- [8] A. Greenbaum, A. Ozcan, *Opt. Express* **20**(3), 3129 (2012); doi: 10.1364/OE.20.003129
- [9] J. Zhang, J. Sun, Q. Chen, J. Li, C. Zuo, *Sci. Rep.* **7**(1), 11777 (2017); doi: 10.1038/s41598-017-11715-x
- [10] L.I. Rudin, S. Osher, E. Fatemi, *Physica D: Nonlinear Phenomena* **60**(1), 259 (1992); doi: 10.1016/0167-2789(92)90242-F